



System dynamics perspective: lack of long-term endogenous feedback accounts for failure of bucket models to replicate slow hydrological behaviors

Xinyao Zhou¹, Zhuping Sheng², Kiril Manevski^{3,6,7}, Yanmin Yang¹, Shumin Han¹, Mathias Neumann Andersen^{3,6}, Qingzhou Zhang⁴, Jinghong Liu^{1,5}, Huilong Li¹, Yonghui Yang¹

¹Key Laboratory of Agricultural Water Resources, Hebei Laboratory of Agricultural Water-Saving, Center for Agricultural Resources Research, Institute of Genetics and Developmental Biology, Chinese Academy of Sciences, Shijiazhuang 050021, China

²Department of Civil Engineering, Morgan State University, Baltimore, MD 21251, USA

10 ³Department of Agroecology, Aarhus University, Tjele 8830, Denmark

⁴Land Resources Exploration Center of Hebei Bureau of Geology and Mineral Exploration and Development (Hebei Mine and Geological Disaster Emergency Rescue Center), Shijiazhuang 050081, China

⁵University of Chinese Academy of Sciences, Beijing 100190, China

⁶Sino-Danish College, University of Chinese Academy of Sciences, Yanqihu Campus, Beijing 101408, China

15 ⁷iClimate – Aarhus University Interdisciplinary Center for Climate Change, Department of Environmental Science, Roskilde 4000, Denmark

Correspondence to: Xinyao Zhou (zhouxy@sjziam.ac.cn) and Yonghui Yang (yonghui.yang@sjziam.ac.cn)

Abstract. Hydrological models with the conceptual tipping bucket and the process-based evapotranspiration models are the most common tools in hydrology. However, these models consistently fail to replicate long-term and slow dynamics of a hydrological system, indicating the need for model augmentation and shift in approach. This study employed an entirely different approach – system dynamics – towards more realistic replication of long-term and slow hydrological behaviors by removing limits of exogenous climate on evapotranspiration and involving endogenous soil water-vegetation feedback loop. Using the headwaters of Baiyang Lake in China as a case study, the mechanisms of slow hydrological dynamics were gradually unraveled from 1982 to 2015 through wavelet analysis, Granger's causality test, and system dynamics. The wavelet analysis and Granger's causality test identified a negative-correlated, bidirectional causal relationship between evapotranspiration and the water budget across distinct climatic periodicities, suggesting a robust endogenous soil water-vegetation feedback structure operating on a long-term scale. The system dynamics approach successfully captured the slow behavior of the hydrological system under both natural and human-intervention scenarios, demonstrating a self-sustained oscillation arising within the system's boundary. Conventional hydrological models, which rely on process-based evapotranspiration models, operate on an instantaneous scale and are thus susceptible to short-time climatic and vegetation physiological variations. This results in inaccurate depletion rate of soil water stock and in turn, can lead to incorrect calculations of other hydrological variables. However, long-term and slow hydrological dynamics typically involves in endogenous state-dependent modulation and feedback related to changes in vegetation structure, thus are insensitive to exogenous disturbances and can be well replicated using system dynamics approach. This insight that the failure of



35 hydrological models to replicate slow dynamics can be attributed to a time-scale mismatch may offer potential solutions for
improving conventional hydrological models.

Short Summary. Conventional bucket-type hydrological models have struggled to accurately replicate slow dynamics,
making model modification a key concern in hydrological science. The system dynamics approach excels at explaining long-
40 term behavioral pattern through the system's endogenous feedback structure. It was employed in a case study and
successfully captured the slow hydrological behaviors. This highlights that the time-scale mismatch can be attributed to the
failure of conventional hydrological models.

1 Introduction

Hydrological models are scientific tools for describing and predicting the processes of the water cycle under the current and
45 the future climate. In the simplest concept, a "bucket" is used to represent the water storage of a catchment, which fills by
rain and empties by evaporation, transpiration and streamflow (Fowler et al., 2020). In spite of the success of this concept in
understanding the physical processes and revealing the physical parameters involved in the hydrological events, the bucket
model has performed poorly against the long-term and multi-year variability of catchment water storage reported in many
50 inaccuracies of the bucket models in replicating slow hydrological behaviors suggest a lack of key mechanisms involved in
the hydrological system. Alongside structural deficiencies (Fowler et al., 2020; Bouaziz et al., 2021), reasons for erratic
model performance also involve data errors (Kuczera et al., 2010; Hulsman et al., 2021), model structural deficiencies
(Fowler et al., 2020; Bouaziz et al., 2021), poor parameterization (Fowler et al., 2016, 2018), or their combination. However,
model structural deficiency likely plays the key role in most cases of poor performance (Fowler et al., 2020).

55 From a hydrological perspective, two main solutions have been proposed to improve the bucket model structure. The first
introduces a "bottomless bucket" to avoid the "minimum possible storage" limit to the bucket, which empties the bucket on a
seasonal basis and restricts the accumulation of water deficit (Fowler et al., 2020). The "bottomless bucket" configuration
better tracks a long-term decline in soil moisture seen, for instance, in Australia during the 13-year "Millennium" drought
desiccating catchments slowly and gradually (Fowler et al., 2021). On the other hand, groundwater usually responds slowly
60 to rainfall variability and the lag time scales are mediated by the hydrogeology of aquifers and the soil physical
characteristics (Hughes et al., 2012; Markovich et al., 2016). Thus, it is suggested that inter-basin groundwater flow should
be incorporated in hydrological models through a new deeper groundwater reservoir to allow models to better reproduce the
long-term storage fluctuations (Bouaziz et al., 2018; Hulsman et al., 2021). Although some aspects are improved by the
model reconfigurations or modifications, other aspects of the hydrology behavior are still not captured or reflected well, for
65 instance those related to the effect of the terrestrial vegetation on the long-term and slow dynamics in hydrological models
(Fowler et al., 2021).



The system dynamics approach assumes that ample time is required for a system to undergo changes (Meadows, 2008) and thus might be a different approach to describe and interpret the mechanism of the ubiquitously long-term and slow variations of the system's hydrology. Different from the conventional viewpoint postulating that the dynamics of a system are primarily driven by exogenous variables, the system dynamics seeks explanations of endogenous structure for the often complex, difficult-to-understand dynamics and "behaviors" (Forrester, 1968). This is because, on one hand, stocks generally change slowly, thus can act as delays, lags, buffers or shock absorbers in the system (Meadows, 2008). On the other hand, systems often have several competing feedback loops operating simultaneously, creating counteracting and compensating pressures in response to exogenous disturbances (Richardson, 2020). Therefore, exogenous drivers might not be able to explain and anticipate a system's main pattern of behaviors, as the cause and the effect are often distant in time and space in dynamically complex systems (Davis, 2003). In spite of the wide application of system dynamics in different areas (Wiener, 1948; Zera, 2002; Hofkirchner and Schafranek, 2011; Seth and Bayne, 2022) and water management (Bai et al., 2021; Simonovic, 2020) in which natural system only plays a minor role, to our knowledge, the concept has rarely been used in hydrology under natural conditions. System dynamics approach may thus open a new avenue to understand the mechanisms of long-term and slow dynamics of hydrological system.

The main aim of this paper was two-fold, to 1) seek the explanation of endogenous structure for the long-term and slow dynamics of catchment water storage with a case study, and 2) test the ability of the system dynamics approach for (re)producing and predicting long-term and slow hydrological dynamics.

2 Methodology

2.1 Study site description

The study area was located at Taihang Mountain in northern China and comprised of the catchments of the rivers Sha, Tang, and Juma (Fig. 1). The climate is semi-arid with continental monsoons, i.e., hot humid summers, and cold dry winters. The average annual temperature, precipitation, and potential evapotranspiration are 7.5 °C, 556 mm, and 1369 mm, respectively (Yang and Mao, 2011; Zeng et al., 2021). The main geologic characteristics of the Taihang Mountain area are "soil and rock dual texture", with thin topsoil of 0.2-0.5 m rich in plant roots and gravel, and a thick 0.5-10 m subsoil of weathered granite gneiss with highly developed fractures (Cao et al., 2022). The three rivers flow into Baiyang Lake, the largest freshwater lake in the North China Plain (Zhuang et al., 2011). Due to prolonged droughts and intensive human interference since the 1980s, the amount of inflow water to the lake has decreased significantly (Fig. S1). This has resulted in a continuous shrinkage of the water body and ecological degradation in the lake area (Han et al., 2020). Despite many efforts quantifying the impacts of climate change and human activities on the dramatic runoff reduction (Zhuang et al., 2011; Hu et al., 2012; Wang et al., 2021), no studies investigated the dynamics of the catchment water storage.

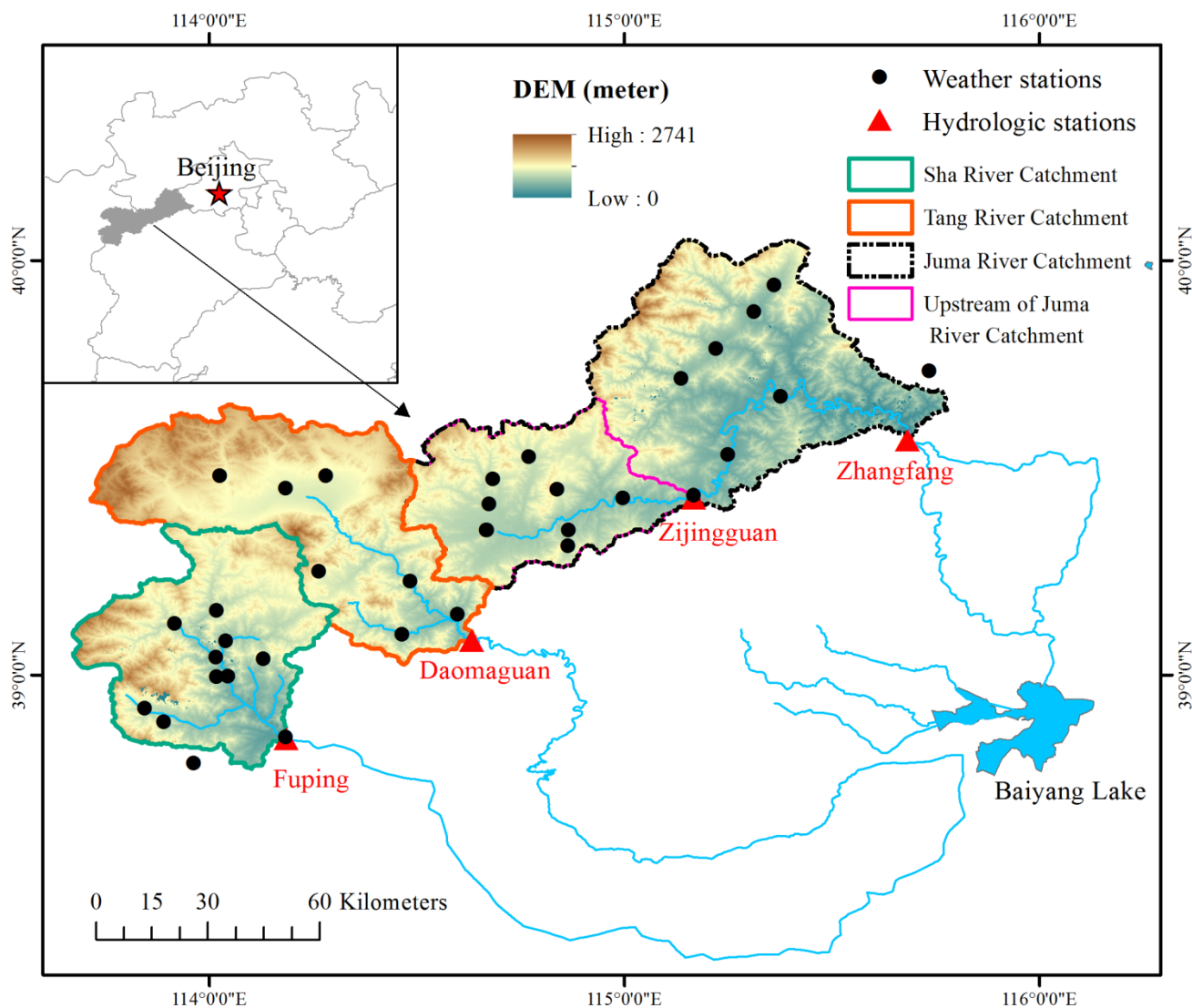


Figure 1: The location of the study area at Baiyang Lake and its headwaters.

2.2 Data compilation and pre-processing

100 Yearly streamflow, rainfall, and actual evapotranspiration data spanning the years 1982-2015 period were compiled for the catchments. Streamflow (Q) from four hydrological stations, viz, Fuping (FP), Daomaguan (DMG), Zijingguan (ZJG), and Zhangfang (ZF) were acquired from the Department of Water Resources of Hebei Province (hereafter the names of the gauge stations was used for representing the catchments; Fig. 1). FP station is located in the Sha River catchment with a drainage area of $2,160 \text{ km}^2$, whereas DMG station is located in the Tang River catchment with a drainage area of $2,704 \text{ km}^2$.

105 ZJG and ZF are the upstream and the downstream stations of the Juma River, respectively, with corresponding drainage



areas of 1,751 and 4,737 km². The unit of streamflow data was in m³ s⁻¹ in the original dataset and was converted to mm year⁻¹ by dividing with the area.

Precipitation data (P; mm year⁻¹) from 34 national weather stations within the study area were downloaded from the China Meteorological Data Sharing Service System (<http://data.cma.cn/>). Actual evapotranspiration (ET; mm year⁻¹) from 1982 to 110 2015 was the average of two gridded remote-sensing based ET data, Numerical Terra-dynamic Simulation Group (NTSG; University of Montata, 2023; 1 km spatial resolution) and ETWatch (8 km resolution for 1984-1989 and 1 km for 1990-2015; the first two years were taken from NTSG). ETWatch (2023) uses the Penman-Monteith model integrated with the SEBAL and the SEBS models (Wu et al., 2008; Wu et al., 2021) and studies show reliable ET estimates over the Haihe Basin where the study area is located (Moiwo et al., 2011; Wu et al., 2012). The NTSG is also a Penman-Monteith model (Zhang et al., 115 2009, 2010). The two ET datasets were comparable with each other.

Catchment water budget (ΔS ; mm year⁻¹) was calculated by the mass balance method subtracting streamflow and actual evapotranspiration from precipitation ($\Delta S = P - Q - ET$). Detrended Total Water Storage Anomalies (TWSA; mm year⁻¹) and surface Soil Moisture (SM; m³ m⁻³) data were used for comparison with ΔS . The TWSA data was based on reconstructed GRACE/GRACE-FO global surface mass changes (land + ocean) from 1979 to 2020 at 0.5° spatial resolution (Li et al., 120 2021). Surface SM data with spatial resolution of 0.25° and temporal coverage from 1979 to 2020 were downloaded from the European Space Agency Climate Change Initiative (ESA CCI) website (Dorigo et al., 2023). This dataset had a high outperformance among satellite-based products (Ma et al., 2019). Comparison of the three datasets were shown in Fig. S2.

Land use data for the Haihe Basin for the 1980s, 1990s, 2000s, and 2010s at 30 m spatial resolution were obtained from the ETWatch (2023) website. From 1980s to 2010s, arable land and high-coverage forest land kept decreasing, while low- 125 coverage vegetation had greatly increased after 2000s (Fig. S3).

Future rainfall data projected by 22 Global Circulation Models (GCMs) were obtained from the Coupled Model Intercomparison Project Phase 6 (CMIP6) website (WCRP, 2023). Details on the 22 GCMs are shown in Table S1. The projected precipitation data from three climatic scenarios under different socio-economic paths, SSP1+RCP2.6, SSP2+RCP4.5, and SSP5+RCP8.5, were used to predict the dynamics of the hydrological system.

130 2.3 Formal data analysis

2.3.1 Wavelet Analysis

Continuous Wavelet Transform (CWT) was employed to preliminarily identify connection patterns among variables in the time series. The wavelet transform has emerged as one of the most promising function transformation methods acting as a time and frequency localization operator (Pathak, 2009). The advantage of the wavelet transform is that it can reflect the 135 evolution over time of non-stationary time series. Here the CWT analysis was used to generate varying coefficients that signify the similarity between the signal and mother wavelets at any specific scale base. The CWT of a function f with respect to the mother wavelet Ψ is defined by Pathak (2009):



$$W_f(a, b) = \frac{1}{\sqrt{|a|}} \int f(t) \Psi\left(\frac{t-b}{a}\right) dt \quad (1)$$

where $W_f(a, b)$ is the wavelet coefficient, a is the wavelet scale associated with dilation and contraction of a wavelet, and

140 b is a time index describing the location of the wavelet in time.

Prior to the analysis, the time series data of P, ET, Q and ΔS were standardized by subtracting the mean and dividing the standard deviation. Afterwards, correlation analysis was conducted based on the CWT coefficients.

2.3.2 Granger's Causality Test

Granger's Causality Test was adopted to decide causal direction of connections among variables. Correlation analysis alone
145 can only tell how "similar" two variables are, however, correlation is neither necessary nor sufficient condition for causality (Sugihara et al., 2012). Inferring causal direction is important for understanding how a complex system works. The Granger's Causality Test is a widely used method to investigate causality between two variables in a time series (Stokes and Purdon, 2017; Shi et al., 2022). For two time series from processes X and Y, it can be said that Y does not Granger-cause X if X, conditional on its own past, is independent of the past of Y (Banerjee et al., 2023). The typical method to test this
150 dependency of two time series involves fitting a vector autoregressive model for X and measuring whether inclusion of Y in that model makes the fitting error significantly lower:

$$y_i = \alpha_0 + \sum_{j=1}^m \alpha_j y_{i-j} + \sum_{j=1}^m \beta_j x_{i-j} + \varepsilon_i \quad (2)$$

where α_j and β_j are the regression coefficients and ε_i is the error term. The test is based on the null hypothesis:

$$H_0: \beta_1 = \beta_2 = \dots = \beta_m = 0$$

155 The X Granger-causes Y when the null hypothesis is rejected.

Further details on the theory behind the Granger's Causality Test, as well as the Matlab toolbox used in this work can be found in Robert (2023).

2.3.3 Dynamics of Hydrological System

Feedback is in the core of the system dynamics concepts (Meadows, 2008; Richardson, 2020). A feedback loop exists when
160 information resulting from certain actions eventually returns in some form, potentially influencing future actions (Richardson, 2020). Feedback loops can be reinforcing or balancing, the former aiming for exponential growth or accelerating collapse, as disequilibrating and destabilizing structures in systems, whereas the latter aiming for stability and resistance to change, for equilibrating or goal-seeking structures in the system (Meadows, 2008). Combined, reinforcing and balancing feedback loops can generate all manners of dynamic patterns. Both feedback loops coexist in the study area. The
165 reinforcing feedback loop can be considered as the change of vegetation structure because the processes tend to self-enhance



once they started. Here, vegetation structure involves non-physiologic components, e.g., change of compositions by growth and mortality (Li et al., 2023). For example, vegetation growth will create a more humid environment for the benefit of its further growth, while vegetation mortality will exacerbate deterioration and trigger a "death spiral" (Bruehlheide et al., 2018). Soil moisture, on the other hand, can interrupt the self-enhancing processes of change in vegetation structure and is thus
 170 considered as a balancing feedback loop. For example, soil moisture approaching the wilting point increases the difficulties of the root to absorb water, causing slower and finally stagnant vegetation growth, and *vice versa* (Stocker et al., 2023).
 How does the interplay between soil moisture and vegetation structure drive the dynamics of the hydrological system? Firstly, every balancing feedback loop has a desired goal used to compared to the actual system state. If a stock level is above or below the goal, the discrepancy between the actual and the desired levels will initiate corrective action and bring
 175 the state of the system back in line with the goal. Here the desired soil moisture was considered as a value within the range between field capacity and wilting point because at this range water can be held in soil and used for vegetation absorption. Secondly, while traditional hydrological models usually use physical process-based models such as the Penman or the Thornthwaite models to calculate ET, the system dynamics approach calculated ET based on its earlier value. This is because there was an implicit vegetation structure stock behind ET. Starting with an initial vegetation structure level, the growth of
 180 new vegetation can be shown as an inflow and mortality of old vegetation as outflow, which would also drive smooth transformation of ET. Since vegetation structure stock can remember the history of changing flows and the growth/mortality of vegetation generally took several years, ET gradually changed and showed a multi-annual scale increase or decrease trend. The equations of the dynamics of hydrological system solved for each year from 1982 to 2015 are:

$$\begin{aligned} \text{TWS}(t) &= \text{SMS}(t) + \text{GWS}(t) + \text{SWS}(t) & (3) \\ \text{SMS}(t) &= \text{SMS}(t-1) + \Delta s(t) * \text{DT} & (4) \\ \Delta s(t) &= [(\text{P}(t) - \text{Qr}(t)) - \text{ET}(t) - \text{RCH}(t)] & (5) \\ \text{DISC}(t) &= [\text{SMS}(t-1) - \text{ESMS}] / \text{DT} & (6) \\ \text{Qr}(t) &= [\text{P}(t) + \text{DISC}(t)] * \text{C1} & (7) \\ \text{ET}(t) &= \text{ET}(t-1) + [\text{VEG}(t) + \text{DISC}(t)] * \text{C2} & (8) \\ \text{RCH}(t) &= [\text{P}(t) * \text{C3} + \text{DISC}(t)] * \text{K}(t) & (9) \\ \text{Qs}(t) &= \text{GWS}(t-1) * \text{C4} / \text{DT} & (10) \\ \text{GWS}(t) &= \text{GWS}(t-1) + \text{RCH}(t) * \text{DT} - \text{Qs}(t) * \text{DT} - \text{GP}(t) * \text{DT} & (11) \\ \text{SWS}(t) &= [\text{Qr}(t) + \text{Qs}(t)] * \text{DT} & (12) \end{aligned}$$

where TWS, SMS, GWS and SWS are, respectively, total water stock, soil moisture stock, groundwater stock, and surface
 195 water stock, all in mm; Δs is the change in water in soil moisture stock in mm year⁻¹; DISC in mm year⁻¹ is the discrepancy between actual (SMS) and desired (expected) soil moisture stock ESMS (mm); P is precipitation inflow in mm year⁻¹ whereas ET, RCH, Qr, and Qs are outflows indicating, respectively, evapotranspiration, recharge, rapid-response runoff, and slow-response runoff (mm year⁻¹). VEG and GP are human activity parameters for, respectively, vegetation-related activities such as reforestation, and groundwater pumpage both in mm year⁻¹, with their value of 0 representing no human influence.



200 C1, C2, C3, and C4 are dimensionless correction coefficients, K is dimensionless response coefficient related to intrinsic permeability and determined by soil type only, and DT is time interval of one year in this study.

3 Results

3.1 Preliminary Identification of Interconnection Pattern

205 The wavelet analysis revealed significant periodicities in the precipitation data for the study area at 7-8th, and 14-15th years of the 1982-2015 period (Fig. S4). The periodicities were consistent with those of the Pacific Decadal Oscillation (PDO), which is the prime driver of interdecadal change in summer rainfall over East China (Nalley et al., 2016; Zhu et al., 2015). Since the late 1990s, the PDO phase shifted from positive to negative mode, corresponding to the decrease in rainfall in the study area (Fig. S5). The self-calibrating Palmer Drought Severity Index (SC-PDSI) and the Standardized Precipitation Evapotranspiration Index (SPEI) calculated from the climatic data in Beijing both showed major dry periods in 1980-1985
210 and 1999-2011 (Zhao et al., 2017). At the same time, streamflow of the headwater of Baiyang Lake significantly decreased, with tipping point occurring in 1998 (Cui et al., 2019; Xu et al., 2019). These information indicated that the study period can be divided into two distinct phases — wet and dry. The wet phase started in 1984 with the lowest wavelet coefficient of precipitation and ended in 2000 with the second lowest coefficient. The dry phase was from 2001 to 2015.

215 Figure 2 showed the comparison of the four signals (P, ET, Q, and ΔS) in the four catchments of the study area. A scale parameter of 8 was used in this study as the highest for the wavelet power spectrum of multi-decadal periodicities (Fig. S4). The P signal in the four catchments regularly fluctuated in the wet phase, while it disappeared in the dry phase with weaker amplitudes and lower frequencies. The Q signal was roughly synchronous with the P signal, with similar amplitude and frequency. The ΔS signal showed in-phase connection with P signal in the wet phase, however, the in-phase connection disappeared in the dry phase. The ET signal was out of phase with the other signals in the wet phase, while in the dry phase,
220 ET signal only opposed the ΔS signal in their phases.

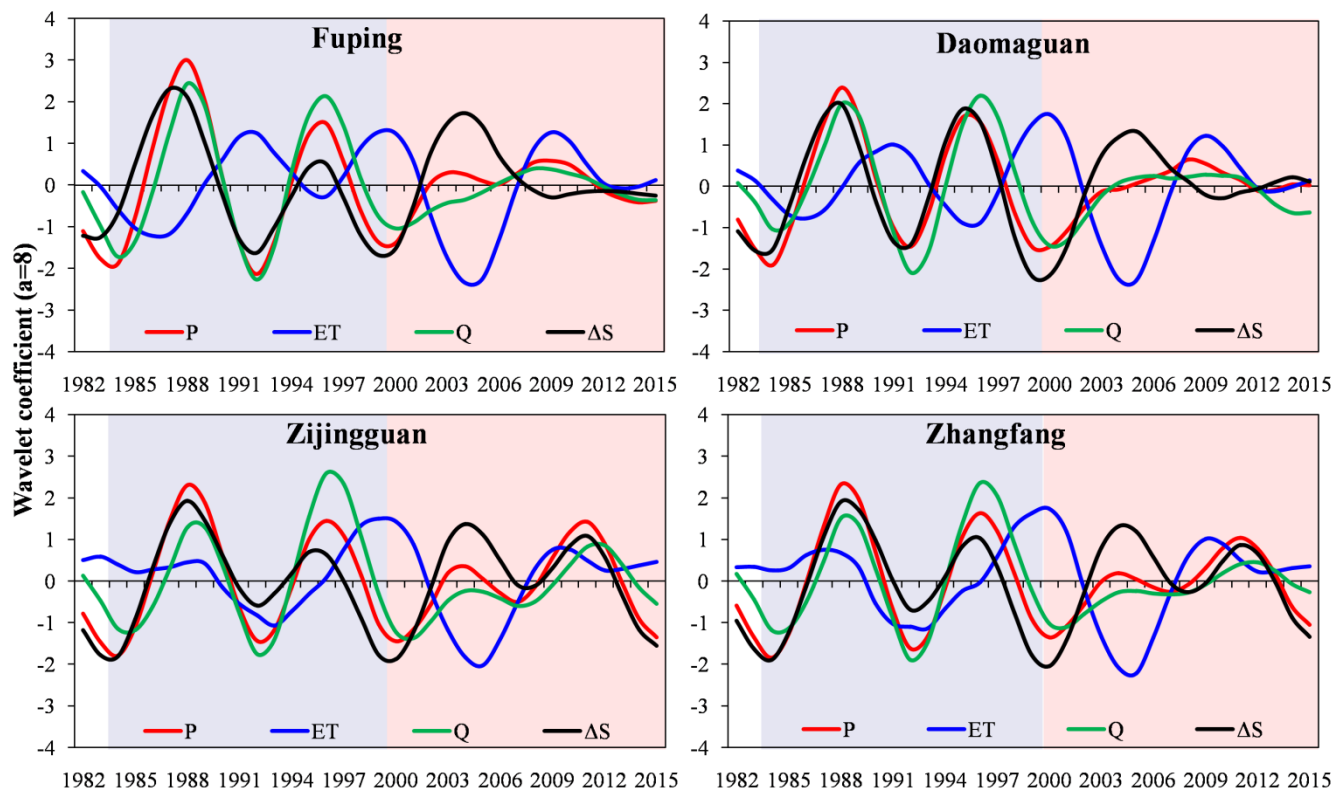


Figure 2: Wavelet coefficients ($a=8$) of four signals (precipitation, P, evapotranspiration, ET, streamflow, Q, and water budget, ΔS) in the four catchments. Blue background indicates wet phase from 1984 to 2000, while the red background indicates dry phase from 2001 to 2015.

225 The correlation analysis (Fig. 3) corroborated the preliminary interconnection results observed in the wavelet analysis, both for the entire study period and the dry/wet phase period. The ET signal was significantly and negatively correlated with the other signals in the wet phase, but only to the ΔS signal in the dry phase. The Q signal significantly and positively correlated to P signal in both dry and wet phases. The ΔS signal in the wet phase showed significant positive correlations with P and Q signals while negative correlation with ET signal in wet phase. In the dry phase, ΔS signal significantly negatively correlated

230 only to the ET signal. Comparable correlations were observed for all four catchments, with larger and more significant values (e.g., ΔS versus ET) for FP and DMG catchments than ZJG and ZF.

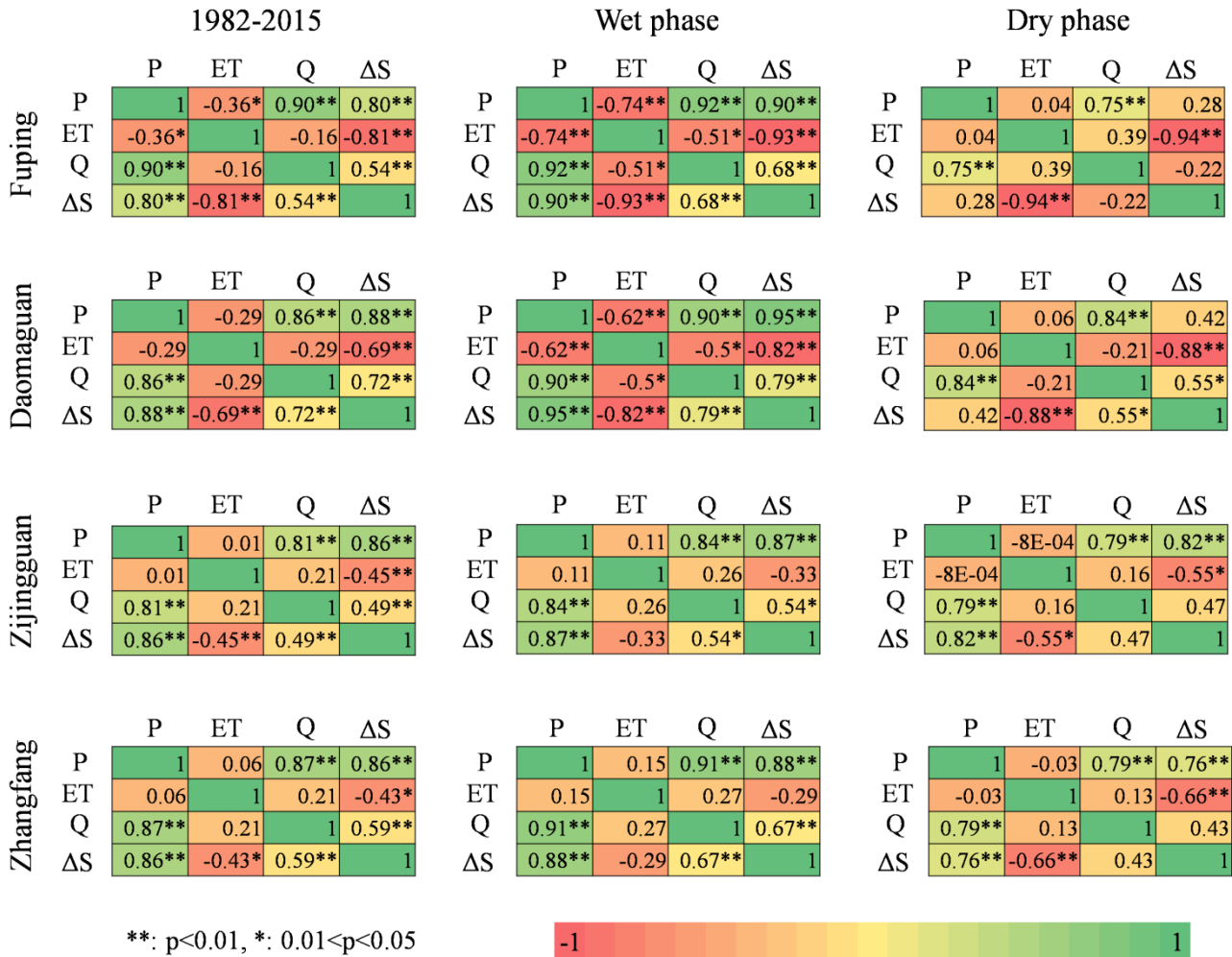


Figure 3: Pearson's correlation matrices for four variables for the whole study period, the wet phase and the dry phase. The calculation is based on wavelet coefficients at scale of 8.

235 3.2 Endogenous structure development of the hydrological system

Understanding causal relationships among variables is very important for developing a correct structure and understanding the behavior of hydrological system which is the base of simulation of system dynamics. Taking FP catchment as example (Fig. 4), the Granger's causality test showed that P does not Granger-cause ET, while it does Granger-cause Q and ΔS . The ET does not Granger-cause Q, while it Granger-causes ΔS . ΔS Granger-causes Q and ET. The results indicated that there is an important trade-off structure between soil moisture and ET in hydrological system.

240

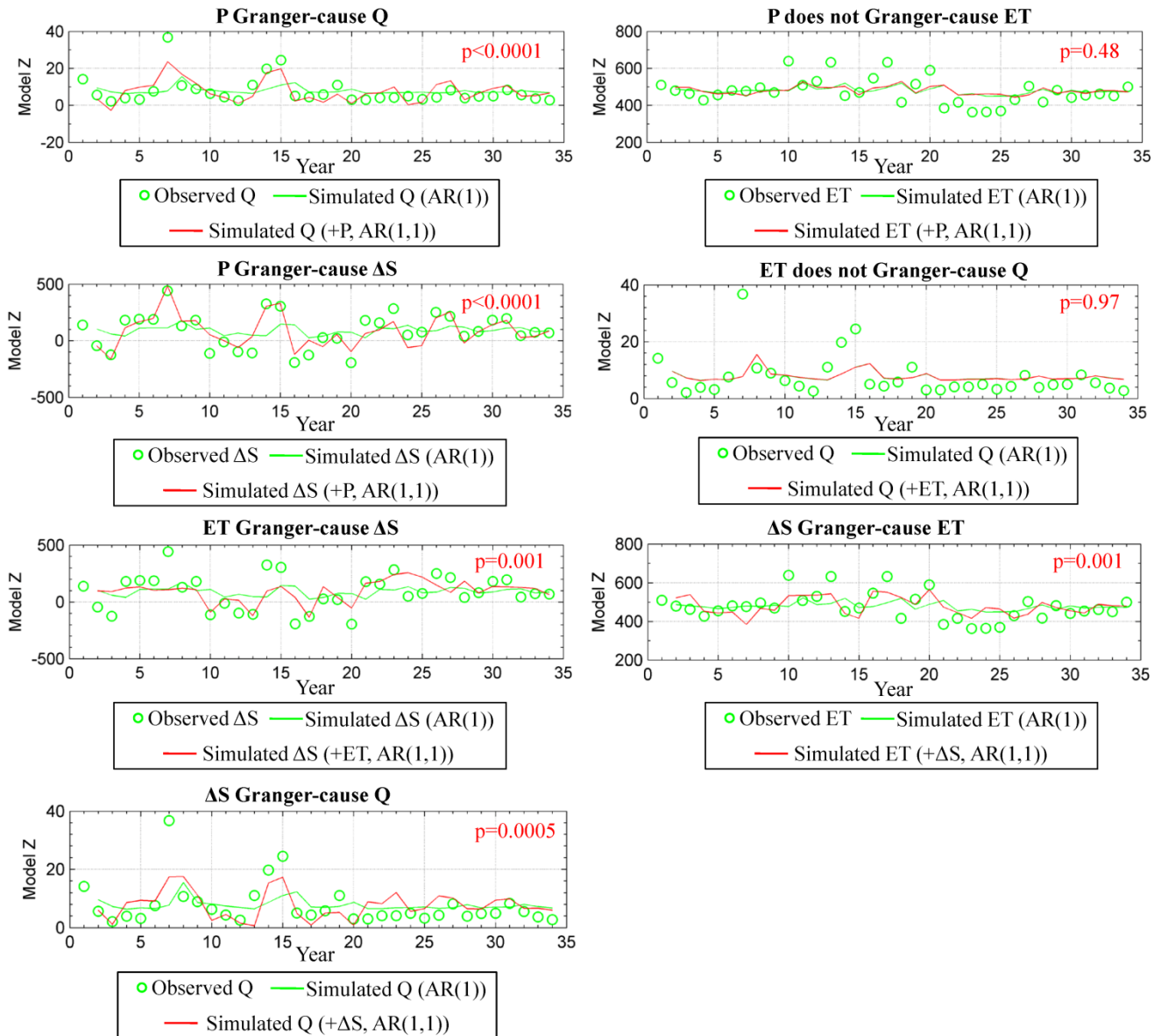
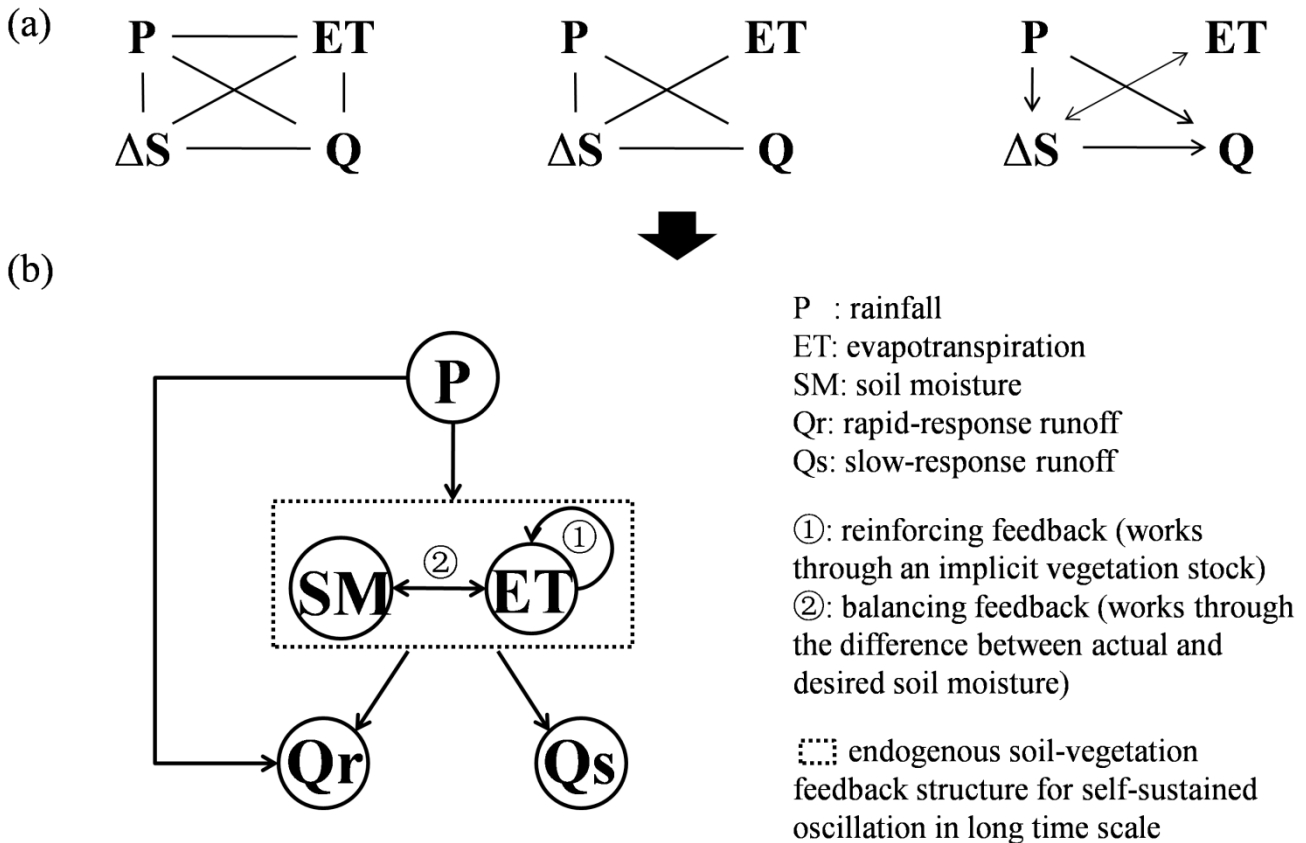


Figure 4: Causal relationships among four hydrological variables of FP catchment. P, Q, ET, and ΔS indicate rainfall, streamflow, evapotranspiration, and water budget respectively. The p-value indicates significance at 95% confidence. Comparable Granger's causality results were seen for the other catchments (not shown for clarity purpose).

245 Therefore, starting from a fully connected network, the links between ET and P or Q could be removed as no causal relationships existed between them, and causal directions were added according to the results above (Fig. 5a). Finally, by combing systematic theory, causal analysis and hydrological knowledge, the final structure and dynamics equations of hydrological system have been derived (Fig. 5b). In the hydrological system, a soil-vegetation feedback structure was at the center position to drive system's dynamic equilibrium, while P was input and Q was influenced by the status of soil moisture.



250

Figure 5: The process of structure development (a) and final structure (b) of hydrological system.

The final structure suggested that the hydrological system boundary was expanded to incorporate ET (vegetation structure) as an endogenous variable. According to system dynamics theory, exogenous variables should have no feedbacks from or interactions with the stocks inside system boundary (Sterman, 2000). For this study, it was appropriate to exclude P outside the system boundary and consider P as the sole source variable because P was insensitive to local surface ET and soil moisture over such a small area (Wei and Dirmeyer, 2019). Meanwhile, ET (vegetation structure) exhibited strong interactions with SM, despite the significant hysteresis effect that decoupled their short-term relationship. Therefore, ET (vegetation structure) should be included as an endogenous variable. Over long time scale, ET (vegetation structure) was SM-dependent and played an important role in maintaining the dynamic equilibrium of SM. The outflow rate of ET (vegetation structure) could be higher under ample soil water while lower under lack of soil water. Treating ET (vegetation structure) as an exogenous variable may lead to inappropriate depletion rate of SM, as current ET (vegetation structure) was often not related to current climate, which in turn caused further miscalculations of hydrological variables in subsequent periods. Incorporating remote-sensing-based vegetation index could improve ET estimation, but data was often difficult to acquire, and predictions for the future could not be made. Additionally, rapid- and slow-response runoff were consider as

255

260

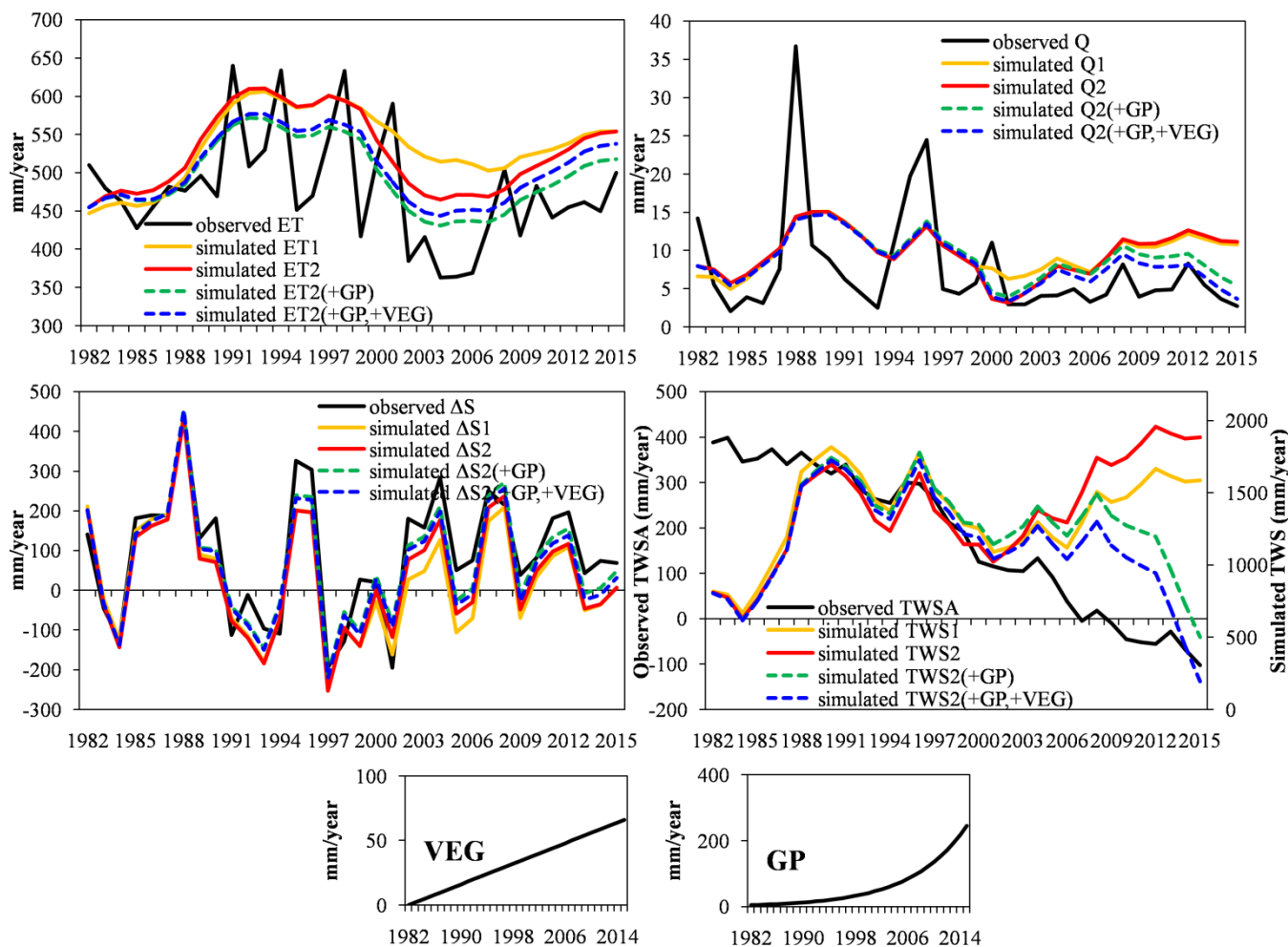


265 sink variables of the hydrological system because their influence on SM and ET could be disregarded once they have
coalesced into the riverbed.

3.3 Dynamics simulation of the hydrological system

According to the dynamics equations (3) - (12), using observed P as input and beginning with an initial soil moisture state,
the dynamics of ET, Q, ΔS ($= P - ET - Q$) and total water storage (soil moisture + groundwater + surface water) of the FP
270 catchment were simulated under both natural and human-intervening scenarios (Fig. 6). The simulated ET captured the long-
term and slow dynamics during the study period, despite the lack of annual fluctuations. Simulated Q and ΔS captured both
the annual fluctuations and the long-term trends (the R-square values of simulated ET, Q, and ΔS are 0.19, 0.21, and 0.82,
respectively). Under natural scenario ($GP = 0$, $VEG = 0$), when a constant ESMS value was used, the discrepancies between
observed and simulated ET and ΔS increased over time. However, if different climatic phases were considered and varying
275 ESMS was adopted to reflect for such climatic periodicity (lower ESMS from 1982-2000 and higher ESMS from 2001-
2015), the discrepancies became smaller (the R-square values of simulated ET, Q, and ΔS are 0.33, 0.17, and 0.85,
respectively). Evident from Figure 6 was the increase in simulated total water storage after 2000 against an observed
anomaly decrease, which was probably caused by human interventions not reflected in the simulation such as groundwater
overexploitation and afforestation activity in the study area since 2000. It is reported that the water use of household sector
280 in FP county mainly relies on groundwater and water demand is projected to increase in the future (Wei and Wang, 2019).
Also, the Taihang Mountain Afforestation Project launched in 1987 and the coverage of vegetation increased 11.2% from
1994 to 2013 (Hu et al., 2017). These two human-intervention scenarios were assumed to linearly increase ET and
exponentially increase groundwater pumpage. When groundwater pumpage scenario was introduced, the simulated ET, ΔS ,
Q and TWS all greatly improved. When the afforestation scenario was added, it pushed further all the simulated values
285 closer to the observations (the R-square values of simulated ET, Q, and ΔS are 0.35, 0.3, and 0.86, respectively).

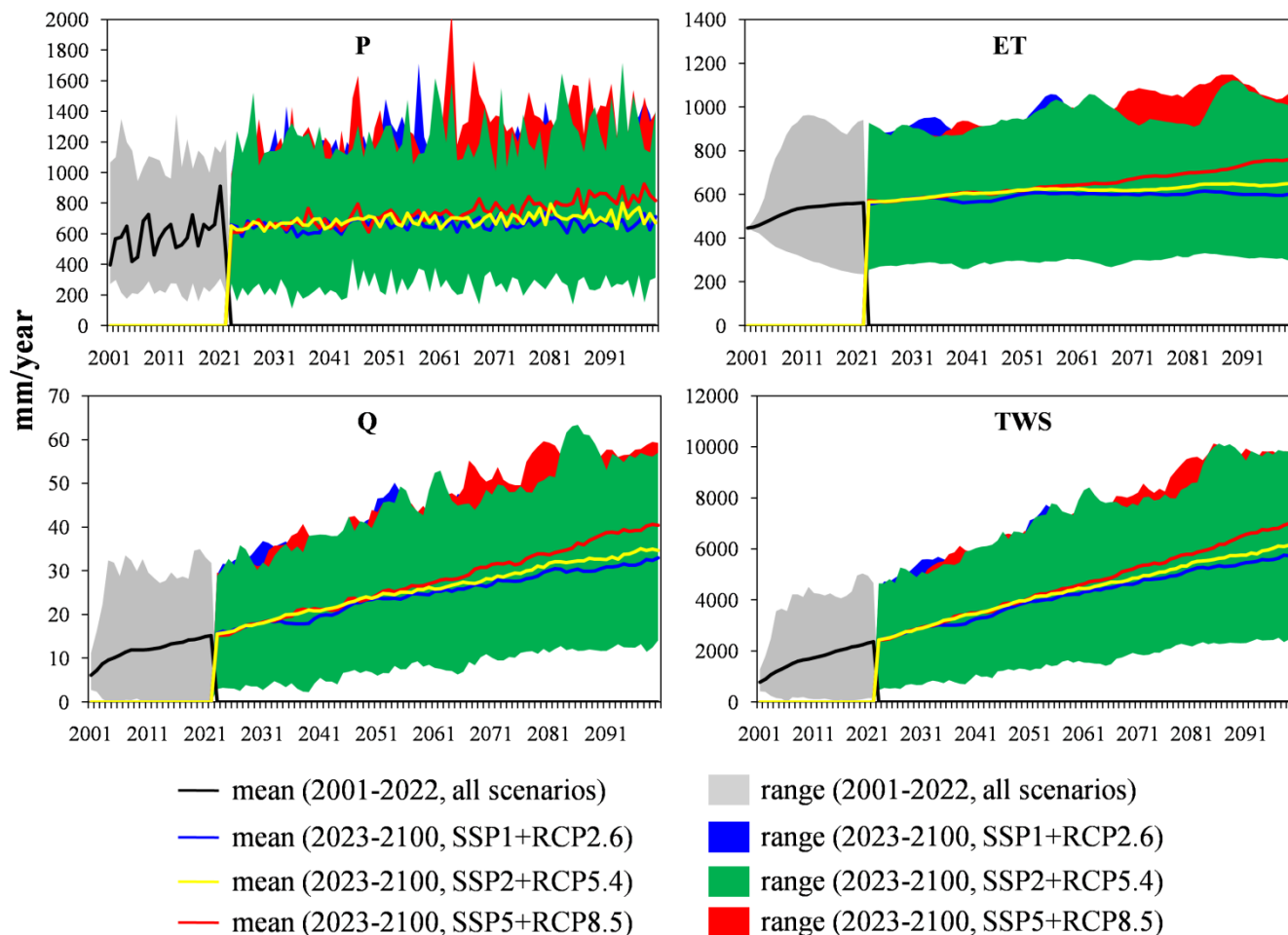
Simulations were conducted for other three catchments with same initial values, parameters, and scenarios (Fig. S6-S8). In
spite of some small discrepancies caused by the parameterization, for instance, the overestimated Q in ZF catchment, the
long-term trends were well captured in all catchments, indicating the robustness of the system dynamic approach. It is thus
important to note that system dynamics approach was insensitive to initial values of variables. In addition, the divergence
290 between observed TWSA and simulated TWS in the first several years was probably caused by the inaccurate reconstruction
of TWSA series because TWS was less likely decreasing under humid climate and marginal groundwater pumpage.



295 **Figure 6: Observed and simulated evapotranspiration (ET), streamflow (Q), water budget (ΔS) and total water storage (TWS) using system dynamics approach for the FP catchment. Yellow and red lines indicate the simulation without human intervention (GP=0 and VEG=0), with respectively fixed and varying desired soil moisture (ESMS). Green dashed line indicates simulation with groundwater pumpage (GP), which increased at an exponential rate. Blue dash line is the simulation with GP and vegetation change (VEG) which is increasing at a linear rate.**

The simulations were also run under different SSP+RCP scenarios for a future climate with probably more severe extreme events – alternate floods and droughts. Here future climate from Baoding station (close to Beijing and study area) was used for representing the whole area. The system dynamics approach showed that Q and TWS will increase in the future under all climatic scenarios, while ET will be comparatively more stable. The projection also pointed on a drought period likely in the 2030s under the low challenging scenario SSP1+RCP2.6 (Fig. 7).

300



305 **Figure 7: Future dynamics of hydrological systems under three climatic scenarios. Future precipitation was from Baoding station close to study area. All the dynamics were simulated with fixed ESMS and without human interventions.**

4 Discussions

4.1 Why is the desired soil moisture higher in the dry phase?

310 Desired soil moisture is a value between wilting point and field capacity, thus it reflects soil water retention capacity of a catchment and higher value suggests higher soil water retention capacity. This is because, firstly, soil holds less water during drought and as a result, there is more space for the soil moisture stock to retain more water. In addition, soil water retention capacity can be further enhanced by the interactions of soil physical, chemical and biological components during drought (Delgado and Gómez, 2017). Physically, drought alters aggregate size fraction with less macro- and more micro-aggregates (Zhang et al., 2019; Su et al., 2020). Also pore network connectivity decreases due to reduced vegetation growth (Nagassa et



al., 2015), which likely increases soil water holding capacity under drought conditions because of poorly connected soil pore
315 network and larger water holding capacity of micropores (Patel et al., 2021). Chemically, the ionic strength of soil solution
can be up to nine orders of magnitude greater in dry soils compared to saturated soils, creating extremely different chemical
environment (Patel et al., 2021). This can cause desorption of different carbon molecules from minerals, and soil organic
carbon (SOM) destabilization (Bailey et al., 2019). Biologically, drought stress reduces population and activity of soil
animals and microbes. This can also destabilize SOM because the microbial community would preferentially consume the
320 more labile/biodegradable organic molecules, leaving behind a more uniform, stable SOM pool (Kaiser et al., 2015).
Furthermore, rainfall pulses in drought period would drive water going deeper because rainfall in dry spells usually occurs as
discrete events (Manzoni et al., 2020).

Overall, the soil water holding capacity of a catchment has enhanced in dry period due to more water storage space and
complex interactions among physical, chemical and biological processes of soils. It makes water easier to be trapped by soil
325 particles rather than utilized by plants, further decreasing evapotranspiration.

4.2 Is the time scales implied by the hydrological approaches?

Physical process-based ET models are widely used in various hydrological models, such as the Penman-Monteith model. It
is generally believed that these physically based equations were derived from experimental data obtained from individual
leaf, and then upscaled to canopy by replacing the leaf-scale resistances with their assumed canopy-scale counterparts
330 (Schymanski and Or, 2017). However, the time scale has not scaled up accordingly alongside the spatial scaling up, thus
such models still operate on instantaneous scale (Chen et al., 2022). In this short time scale, ET is sensitive to environmental
turbulent diffusion (characterized by climate data) and vegetation physiological processes (e.g., leaf expansion and
abscission). As ET is a crucial variable in hydrological models, the climate-sensitive hydrological behaviors have also been
reproduced due to this short-term mechanism.

335 In the long time scale, the climatic and physiological influence becomes minimal as climate over a region is generally stable
and changes slowly over time, while leaves undergo regular cycles of unfolding and falling every year. Consequently,
vegetation structure change, such as tree growth and mortality, has become significant factors influencing ET over climate.
The accessibility to water and the age of trees are the most critical factors influencing tree growth and mortality. And
significantly long time delays are common in both situations; for instance, a tree may take several decades to grow or die,
340 and soil water may take several years to deplete or replenish. System dynamics thus becomes a useful tool aiming to capture
long-term dynamics by focusing on endogenous explanations for long-term dynamics and including crucial feedback loops.
A broad model boundary that incorporates important feedbacks is more important than specifying numerous details for
individual components (Davis, 2003). Therefore, persistent hydrological shifts and especially flow reductions such as those
caused by the increasing enduring multi-year drought can only be described accurately with the system dynamics approach.
345 One should carefully choose suitable tool according to their problems.



5. Conclusions

Using wavelet analysis, Granger's causality test, and ultimately the system dynamics approach for the headwater of Baiyang Lake, China as an example, this study aimed to investigate the mechanism of long-term, slow variation of a hydrological system based on four observed variables (precipitation, ET, streamflow and water budget) during the period of 1982-2015.

350 Unique improved and transferable understanding was achieved on how a hydrological system functions slowly, as summarized below:

(1) There was constantly negative correlations between evapotranspiration and water budget regardless of climatic periodicity, indicating the soil-vegetation feedback structure acted as the central role in the hydrological system. Meanwhile, the correlations between the two factors and other variables differed in wet and dry phases, for instance, Q significantly and
355 positively correlated to water budget in the wet phase and lost the link in the dry phase, implying the interconnections between the pivotal structure and other variables were flexible and could change over time.

(2) Water budget and ET Granger-caused each other, suggesting a bidirectional causal effect in the soil-vegetation feedback structure. Self-enhanced vegetation growth process played a dominant role in driving the hydrological system under ample soil water, whereas soil moisture dominated and balanced the process by forcing vegetation to die under lack of soil water.
360 The endogenous soil-vegetation feedback structure guaranteed the dynamic equilibrium of soil moisture within a range and caused the slow changes of hydrological system because growth and mortality of vegetation generally took years.

(3) The system dynamics approach involved endogenous soil-vegetation feedback structure to successfully capture the long-term and slow behavior of hydrological system under both natural and human-intervention scenarios. The simulations better reflected observed patterns when varying desired soil moisture was adopted, suggesting soil had higher water retention
365 capacity in the dry phase than wet phase. Meanwhile, reforestation and groundwater pumpage scenarios greatly improved the simulations of all hydrological variables.

In conclusion, the system dynamics approach provides a different view on the long-term and endogenous processes in a hydrological system, and better represents the observed functions of hydrological system compared to bucket models. With quantitative insights on hydrological system behavior, we could advance a new era of hydrological science.

370 Financial support:

This work was supported by two grants of the National Natural Science Foundation of China (Grant no. 4217012319 and 42301036).

Data Availability

The gridded data are available in the main text and the catchment-scale data can be obtained by contacting Xinyao Zhou
375 (zhouxu@sjziam.ac.cn) and Yonghui Yang (yonghui.yang@sjziam.ac.cn).



Author contributions

Xinyao Zhou: Conceptualization, Methodology, Visualization, Writing — Original draft preparation. Zhuping Sheng, Kiril Manevski, Mathiasn Andersen, and Yonghui Yang: Supervision, Writing — Review & Editing. Yanming Yang, Shumin Han, Jinghong Liu, Qingzhou Zhang and Huilong Li: Resources.

380 Competing interests

The contact author has declared that none of the authors has any competing interests.

References

- Banerjee, A., Chandra, S., and Ott, E., 2023. Network inference from short, noisy, low time-resolution, partial measurements: Application to *C. elegans* neuronal calcium dynamics. *PNAS*, 120(12), e2216030120.
- 385 Bai, Y., Langarudi, S.P., and Fernald, A.G., 2021. System dynamics modeling for evaluating regional hydrologic and economic effects of irrigation efficiency policy. *Hydrology*, 8(2), 61.
- Bailey, V.L., Pries, C.H., and Lajtha, K., 2019. What do we know about soil carbon destabilization? *Environmental Research Letter*, 14, 083004.
- Bouazia, L., Weerts, A., Schellekens, J., et al., 2018. Redressing the balance: quantifying net intercatchment groundwater
390 flows. *Hydrology and Earth System Sciences*, 22, 6415-6434.
- Bouaziz, L.J.E., Fencia, F., Thirel, G., et al., 2021. Behind the scenes of streamflow model performance. *Hydrology and Earth System Sciences*, 25, 1069-1095.
- Bruehlheide, H., Dengler, J., Purschke, O., et al., 2018. Global trait-environment relationships of plant communities. *Nature Ecology & Evolution*, 2, 1906-1917.
- 395 Cao, J., Yang, H., and Zhao, Y., 2022. Experimental analysis of infiltration process and hydraulic properties in soil and rock profile in the Taihang Mountain, North China. *Water Supply*, 22(2), 1691-1703.
- Chen, J., Wilson, C.R., Tapley, B.D., Scanlon, B., and Güntner, A., 2016. Long-term groundwater storage change in Victoria, Australia from satellite gravity and in situ observations. *Global and Planetary Change*, 139, 56-65.
- Chen, H., Huang, J.J., Dash, S.S., Wei, Y., and Li, H., 2022. A hybrid deep learning framework with physical process
400 description for simulation of evapotranspiration. *Journal of Hydrology*, 606, 127422.
- Creutzfeldt, B., Ferré, T., Troch, P., et al., 2012. Total water storage dynamics in response to climate variability and extremes: Inference from long-term terrestrial gravity measurement. *Journal of Geophysical Research*, 117, D08112.
- Cui, H., Xiao, W., Zhou, Y., et al., 2019. Runoff responses to climate change and human activities in the upper Daqing River Basin. *South-to-North Water Transfers and Water Science & Technology*, 17(4), 54-62. (in Chinese)



- 405 Davis, G.B., 2003. Systems Approach. Encyclopedia of Information Systems, Elsevier, <https://doi.org/10.1016/B0-12-227240-4/00178-7>.
- Delgado, A., and Gómez, J.A., 2017. The soil. Physical, chemical and biological properties. Principles of Agronomy for Sustainable Agriculture, Springer, Chapter 2, pp15-26.
- Dorigo, W., Preimesberger, W., Moesinger, L., et al., 2023. ESA Soil Moisture Climate Change Initiative
410 (Soil_Moisture_cci): Version 07.1 data collection. NERC EDS Centre for Environmental Data Analysis, 03 May 2023, doi:
10.5285/ea3eb0714dc6402b905fe9f7ee50dbbc.
- ETWatch, 2023. Haihe Basin ET Dataset and Haihe Basin Landuse. www.etwatch.cn. Available at 2023-9-28.
- Fowler, K., Peel, M., Western, A., et al., 2016. Simulating runoff under changing climatic conditions: Revisiting an apparent deficiency of conceptual rainfall-runoff models. *Water Resources Research*, 52, 1820-1846.
- 415 Fowler, K., Pell, M., Western, A., and Zhang, L., 2018. Improved rainfall-runoff calibration for drying climate: Choice of objective function. *Water Resources Research*, 54.
- Fowler, K., Knoben, W., Peel, M., et al., 2020. Many commonly used rainfall-runoff models lack long, slow dynamics: Implications for runoff projections. *Water Resources Research*, 56, e2019WR025286.
- Fowler, K.J.A., Coxon, G., Freer, J.E., et al., 2021. Towards more realistic runoff projections by removing limits on
420 simulated soil moisture deficit. *Journal of Hydrology*, 600, 126505.
- Forrester, J.W., 1968. Principles of Systems. Pegasus Communications: Waltham, MA.
- Han, Q., Tong, R., Sun, W., et al., 2020. Anthropogenic influences on the water quality of the Baiyangdian Lake in North China over the last decade. *Science of the Total Environment*, 701, 134929.
- Hofkirchner, W., and Schafranek, M., 2011. General System Theory. *Handbook of the Philosophy of Science*, 10:
425 Philosophy of complex systems.
- Hu, S., Liu, C., Zheng, H., et al., 2012. Assessing the impacts of climate variability and human activities on streamflow in the water source area of Baiyangdian Lake. *Journal of Geographical Sciences*, 22(5), 895-905.
- Hu, Y., Zhai, H., and Tian, Y., 2017. Analysis on sustainability of Taihang Mountain Greening Program construction. *Forestry Economics*, 2017(9), 48-52. (in Chinese)
- 430 Hughes, J.D., Petrone, K.C., and Silberstein, R.P., 2012. Drought, groundwater storage and stream flow decline in southwestern Australia. *Geophysical Research Letters*, 39(3).
- Hulsman, P., Hrachowitz, M., and Savenije, H.H.G., 2021. Improving the representation of long-term storage variations with conceptual hydrological models in data-scarce regions. *Water Resources Research*, 57, e2020WR028837.
- Jing, W., Yao, L., Zhao, X., et al., 2019. Understanding terrestrial water storage declining trends in the Yellow River Basin.
435 *Journal of Geophysical Research: Atmospheres*, 124, 12963-12984.
- Kaiser, M., Kleber, M., and Berhe, A.A., 2015. How air-drying and rewetting modify soil organic matter characteristics: an assessment to improve data interpretation and inference. *Soil Biology & Biochemistry*, 80, 324-340.



- Kuczera, G., Renard, B., Thyer, M., and Kavetski, D., 2010. There are no hydrological monsters, just models and observations with large uncertainties! *Hydrological Sciences Journal*, 55(6), 980-991.
- 440 Li, F., Kusche, J., Chao, N., et al., 2021. Long-term (1979-present) total water storage anomalies over the global land derived by reconstructing GRACE data. *Geophysical Research Letters*, 48, e2021GL093492.
- Ma, H., Zeng, J., Chen, N., et al., 2019. Satellite surface soil moisture from SMAP, SMOS, AMSR2 and ESA CCI: A comprehensive assessment using global ground-based observations. *Remote Sensing of Environment*, 231, 111215.
- Manzoni, S., Chakrawal, A., Fischer, T., et al., 2020. Rainfall intensification increases the contribution of rewetting pulses to
445 soil heterotrophic respiration. *Biogeosciences*, 17, 4007-4023.
- Markovich, K.H., Maxwell, R.M., and Fogg, G.E., 2016. Hydrogeological response to climate change in alpine hillslopes. *Hydrological Processes*, 30(18), 3126-3138.
- Meadows, D.H., 2008. *Thinking in Systems: A Primer*. Chelsea Green Publishing.
- Moiwo, J.P., Yang, Y., Yan, N., and Wu, B., 2011. Comparison of evapotranspiration estimated by ETWatch with that
450 derived from combined GRACE and measured precipitation data in Hai River Basin, North China. *Hydrological Sciences Journal*, 56(2), 249-267.
- Nalley, D., Adamowski, J., Khalil, B., et al., 2016. Inter-annual to inter-decadal streamflow variability in Quebec and Ontario in relation to dominant large-scale climate indices. *Journal of Hydrology*, 536, 426-446.
- Negassa, W.C., Guber, A.K., Kravchenko, A.N., et al., 2015. Properties of soil pore space regulate pathways of plant residue
455 decomposition and community structure of associated bacteria. *PLoS ONE*, 10, 1-22.
- Patel, K.F., Fansler, S.J., Compbell, T.P., et al., 2021. Soil texture and environmental conditions influence the biogeochemical responses of soils to drought and flooding. *Communications Earth & Environment*, 2:127.
- Pathak, R.S., 2009. *The wavelet transform*. Atlantis Studies in Mathematics for Engineering and Science. Series Editor: Chui, C.K. Atlantis Press, Paris, France.
- 460 Richardson, 2020. *Core of System Dynamics*. *System Dynamics - Theory and Application*. A Volume in the Encyclopedia of Complexity and Systems Science, Second Edition. Springer.
- Robert, 2023. *Granger_Cause_1* (https://www.mathworks.com/matlabcentral/fileexchange/59390-granger_cause_1), MATLAB Central File Exchange.
- Schymanski, S.J., and Or, D., 2017. Leaf-scale experiments reveal an important omission in the Penman-Moneith equation.
465 *Hydrology and Earth System Sciences*, 21, 685-706.
- Seth, A.K., and Bayne, T., 2022. Theories of consciousness. *Nature Reviews: Neuroscience*, 23, 439-452.
- Shao, R., Zhang, B., He, X., et al., 2021. Historical water storage changes over China's Loess Plateau. *Water Resources Research*, 57, e2020WR028661.
- Shi, H., Zhao, Y., Liu, S., et al., 2022. A new perspective on drought propagation: causality. *Geophysical Research Letters*,
470 49, e2021GL096758.



- Simonovic, S.P., 2020. Application of the systems approach to the management of complex water systems. *Water*, 12(10), 2923.
- Sterman, J.D., 2000. *Business Dynamics: System thinking and modeling for a complex world*. McGraw-Hill Education.
- Su, X., Su, X., Yang, S., et al., 2020. Drought changed soil organic carbon composition and bacterial carbon metabolizing patterns in a subtropical evergreen forest. *Science of the Total Environment*, 76(2020), 139568.
- 475 Sugihara, G., May, R., Ye, H., et al., 2012. Detecting causality in complex ecosystems. *Science*, 338(6106), 496-500.
- Stokes, P.A., and Purdon, P.L., 2017. A study of problems encountered in Granger causality analysis from a neuroscience perspective. *PNAS*, E7063-E7072.
- Stocker, B.D., Tumber-Dávila, S.J., Konlgs, A.G., et al., 2023. Global patterns of water storage in the rooting zones of vegetation. *Nature Geoscience*, 16, 250-256.
- 480 University of Montana, 2023. URL: <https://www.umt.edu/numerical-terradynamic-simulation-group/default.php>. Available at 2023-9-28.
- Wang, H., Lv, X., and Zhang, M., 2021. Sensitivity and attribution analysis based on the Budyko hypothesis for streamflow change in Baiyangdian catchment, China. *Ecological Indicators*, 121, 107221.
- 485 Wei, C., and Wang, H., 2019. Research of water supply strategies in Fuping county. *Design of Water Resources & Hydroelectric Engineering*, 38(4), 21-23. (in Chinese)
- Wei, J., and Dirmeyer, P.A., 2019. Sensitivity of land precipitation to surface evapotranspiration: a nonlocal perspective based on water vapor transport. *Geophysical Research Letters*, 46(21), 12588-12597.
- WCRP, 2023. World Climate Research Programme. Department of Energy. URL: <http://esgf-node.llnl.gov/search/cmip6/>.
- 490 Available at 2023-9-28.
- Wiener, N., 1948. *Cybernetics: or Control and Communication in the Animal and the Machine*. MIT Press.
- Wu, B., Xiong, J., and Yan, N., 2008. ETWatch for monitor regional evapotranspiration with remote sensing. *Advances in Water Science*, 19(5), 671-678.
- Wu, B., Yan, N., Xiong, J., et al., 2012. Validation of ETWatch using field measurements at diverse landscapes: A case study in Hai Basin of China. *Journal of Hydrology*, 436-437, 67-80.
- 495 Wu, F., Wu, B., Zhu, W., et al., 2021. ETWatch cloud: APIs for regional actual evapotranspiration data generation. *Environmental Modelling & Software*, 145, 105174.
- Xu, Q., Cheng, W., Sun, T., et al., 2019. The influence of climate factors on runoff of major rivers in upper reaches of Baiyangdian lake. *Journal of Hebei Agricultural University*, 42(2), 110-115. (in Chinese)
- 500 Yang, Z., and Mao, X., 2011. Wetland system network analysis for environmental flow allocations in the Baiyangdian Basin, China. *Ecological Modelling*, 222(20-22), 3785-3794.
- Zera, D.A., 2002. What is a system and a system perspective? *Educational Horizons*, 81(1), 18-20.
- Zeng, Y., Zhao Y., and Qi, Z., 2021. Evaluating the ecological state of Chinese Lake Baiyangdian (BYD) based on ecological network analysis. *Ecological Indicators*, 127, 107788.



- 505 Zhang, K., Kimball, J.S., Mu, Q., Jones, L.A., Goetz, S.J., Running, S.W., 2009. Satellite based analysis of northern ET trends and associated changes in the regional water balance from 1983 to 2005. *Journal of Hydrology*, 379, 92–110.
- Zhang, K., Kimbal, J.S., Nemani, R.R., Running, S.W., 2010. A continuous satellite-derived global record of land surface evapotranspiration from 1983 to 2006. *Water Resource Research*, 46, W09522.
- Zhang, Q., Shao, M., Jia, X., et al., 2019. Changes in soil physical and chemical properties after short drought stress in semi-
510 humid forests. *Geoderma*, 338(2019), 170-177.
- Zhao, H., Gao, G., An, W., et al., 2017. Timescale differences between SC-PDSI and SPEI for drought monitoring in China. *Physics and Chemistry of the Earth*, 102, 48-58.
- Zhu, Y., Wang, H., Ma, J., et al., 2015. Contribution of the phase transition of Pacific Decadal Oscillation to the late 1990s' shift in East China summer rainfall. *Journal of Geophysical Research: Atmospheres*, 120, 8817-8827.
- 515 Zhuang, C., Ouyang, Z., Xu, W., et al., 2011. Impacts of human activities on the hydrology of Baiyangdian Lake, China. *Environmental Earth Sciences*, 62, 1343-1350.